

EVALUATION OF THE CSM-CROPSIM-CERES-WHEAT MODEL AS A TOOL FOR CROP WATER MANAGEMENT

K. R. Thorp, D. J. Hunsaker, A. N. French, J. W. White, T. R. Clarke, P. J. Pinter Jr.

ABSTRACT. *Development and implementation of improved methodologies for crop water management will conserve valuable water resources in agricultural regions that depend on irrigation. To address this problem for conditions in central Arizona, we have evaluated the CSM-CROPSIM-CERES-Wheat model using measured wheat growth and soil water data from plot-level irrigation scheduling experiments conducted during the winters of 2003-2004 and 2004-2005. During each season, wheat plots were managed using two FAO-56-based irrigation scheduling approaches at three planting densities (~75, ~150, and ~300 plant m⁻²) and at two nitrogen application rates (~80 and ~215 kg ha⁻¹ year⁻¹). For these treatments, the calibrated model simulated wheat yield with relative root mean squared errors (RRMSE) of 7.4% and 1.7% for the 2003-2004 and 2004-2005 seasons, respectively. Time series plots of measured and simulated Zadoks number, leaf number, leaf mass, stem mass, spike mass, and green leaf area index demonstrated favorable wheat development and growth responses to experimental treatments and seasonal weather and management variability. The model was able to quantify average soil water contents in eight soil layers to a depth of 210 cm with RRMSEs ranging from 3.3% to 18.9% for the 2003-2004 season and from 2.7% to 11.3% for the 2004-2005 season. Evapotranspiration was simulated with RRMSEs of 2.4% and 3.2% for the 2003-2004 and 2004-2005 seasons, respectively. Deficiencies were demonstrated in the ability of the model's automatic irrigation routines to reproduce the FAO-56 irrigation schedules devised during field experimentation. With further development, the CSM-CROPSIM-CERES-Wheat model could become a valuable central component for decision tools designed to evaluate alternative water management scenarios and improve water management for irrigated agricultural systems.*

Keywords. *Arizona, CERES-Wheat, Crop model, CROPSIM, CSM, DSSAT, Evaluation, Irrigation scheduling, Simulation, Wheat.*

Growing competition for limited water resources in the arid and semi-arid regions of the western U.S. has created a need for improved crop water management in the agricultural sector. Effective on-farm water management strategies should address the amount, timing, and spatial location of irrigation water to be applied. Several different approaches exist for studying crop water use and developing water management strategies for crops, including direct measurement of soil water contents or soil matric potential; measurement or estimation of actual crop evapotranspiration (ET_c); plant-based assessments of leaf water potential, canopy temperature, or sap flow; and modeling techniques based on mass balance principles (Itier et al., 1996). Many researchers and some practitioners use a combination of these scientific approaches to understand and manage the hydrology of irrigated agricultural systems.

However, on-farm water management decisions are often complicated by issues unrelated to the specific crop water needs. For example, inadequate water supplies, issues with regional water delivery mechanisms, or unfavorable political decisions concerning water rights may all affect water availability at the farm level, which will in turn affect on-farm water management decisions (Pereira et al., 2002). A robust tool for improvement of on-farm water management must therefore provide information on crop water requirements as well as provide assessments of alternative management scenarios during times of inadequate water supply.

Crop systems models (Jones et al., 2003) are well suited for rapid assessment of on-farm water management alternatives, which may be particularly important for situations where water availability is highly uncertain. Crop systems models are process-oriented computer simulation models that simulate the daily water, nutrient, and plant growth processes occurring within agricultural cropping systems throughout the growing season. These models can be used to simulate the collective effects of meteorological conditions, soil properties, cultivar characteristics, and management practices on crop growth, development, water use, and yield. Several previous studies report diverse applications of crop systems models to understand crop growth and yield responses to water management alternatives. Stockle and James (1989) simulated the effects of four levels of deficit irrigation on corn yield in central California and found that deficit irrigation provided a better net economic benefit than full irrigation in some cases. Lobell and Ortiz-Monasterio (2006)

Submitted for review in February 2009 as manuscript number SW 7899; approved for publication by the Soil & Water Division of ASABE in December 2009.

The authors are **Kelly R. Thorp**, ASABE Member Engineer, Agricultural Engineer, **Douglas J. Hunsaker**, ASABE Member Engineer, Agricultural Engineer, **Andrew N. French**, Physical Scientist, **Jeffrey W. White**, Plant Physiologist, **Thomas R. Clarke**, Former Physical Scientist, and **Paul J. Pinter, Jr.**, Former Research Biologist, USDA-ARS U.S. Arid Land Agricultural Research Center, Maricopa, Arizona. **Corresponding author:** Kelly R. Thorp, USDA-ARS U.S. Arid Land Agricultural Research Center, 21881 N. Cardon Lane, Maricopa, AZ 85138; phone: 520-316-6375; fax: 520-316-6330; e-mail: kelly.thorp@ars.usda.gov.

used the CERES–Wheat model to evaluate the impact of reduced irrigations on spring wheat yields in the Yaqui Valley of Mexico and concluded that yield reductions from reduced irrigation depended largely on precipitation. CERES–Wheat simulations by Arora et al. (2007) for conditions in Punjab, India, demonstrated that grain yield and water productivity were highly influenced by the capacity of extractable soil water. Other researchers have developed systems models as tools for irrigation scheduling (George et al., 2004; Cai et al., 2009) and for regional assessment of irrigation water demand (Guerra et al., 2004; Santhi et al., 2005). These studies demonstrate the versatility of crop systems models for addressing diverse problems related to crop water management.

Before applying a crop systems model to answer crop water management questions, it must be adequately tested against field measurements to ensure that the simulation results are reasonable. Thus, crop systems modeling and agronomic experimentation are complementary endeavors, and the ongoing effort to marry these two pursuits is an important agricultural research direction. During the winters of 2003–2004 and 2004–2005 in Maricopa, Arizona, intensive field experiments were conducted to compare two FAO–56 irrigation scheduling methods (Allen et al., 1998) for wheat (*Triticum aestivum* L.). One scheduling method used an “average” seasonal crop coefficient curve for typical growing seasons, and the other used crop coefficients tailored specifically for each growing season based on canopy spectral reflectance measurements (Hunsaker et al., 2007a, 2007b). Irrigations were scheduled for wheat at three plant population levels and two nitrogen application rates. Since agronomic and soil moisture measurements were intensively collected throughout each field experiment, the measured dataset is of great value for evaluating a crop systems model as a tool for studying crop water management in Arizona. The objectives of this work were (1) to calibrate and validate the CSM–CROPSIM–CERES–Wheat model using two years of measured data from wheat irrigation scheduling experiments at Maricopa, Arizona, and (2) to evaluate the ability of the model’s automatic irrigation routine to reproduce the FAO–56 irrigation schedule developed during each field experiment. Current and previous versions of this wheat growth model have been widely used to simulate the collective effect of cultivar characteristics, management practices, weather, and soil conditions on the growth, development, and yield of wheat plants, and the model has been shown to perform adequately for a wide selection of wheat varieties, climatic conditions, and soil types around the world (Chipanshi et al., 1999; Bannayan et al., 2003; Nain et al., 2004; Rinaldi, 2004; Lobell and Ortiz–Monasterio, 2006; Arora et al., 2007). Specifically for conditions in Arizona, the CERES–Wheat model, a predecessor to the current version, has been evaluated using a dataset collected during the Free–air Carbon Dioxide Enrichment (FACE) experiments from 1992 to 1994 (Tubiello et al., 1999).

MATERIALS AND METHODS

CSM–CROPSIM–CERES–WHEAT

CSM–CROPSIM–CERES–Wheat is one of the plant growth modules within the Cropping System Model (CSM; ver. 4.5.0.036; Jones et al., 2003), as provided in the Decision Support System for Agrotechnology Transfer (DSSAT). It is

a computer program that utilizes carbon, nitrogen, and water balance principles to simulate the processes that occur during the growth and development of wheat plants within an agricultural system. The model calculates crop growth and development within a homogeneous area on a daily time step. Crop development proceeds through nine growth stages based on heat unit accumulation from planting to harvest, and leaf numbers are computed during vegetative growth stages. Carbon assimilation is computed as a function of incoming solar radiation, leaf area index (LAI), plant population, the canopy extinction coefficient, and radiation use efficiency. Assimilated carbon is then partitioned to various plant parts, including leaves, stems, spikes, chaff, grain, and roots. Simulated plant growth responds to variation in management practices, crop cultivars, soil properties, and meteorological conditions. Management inputs required for model execution include plant population, row spacing, seed depth, planting and harvest dates, fertilizer application amounts and dates, and irrigation application amounts and dates. Cultivar parameters are used to define vernalization requirements, daylength sensitivity, radiation use efficiency, heat units needed to progress through growth stages, and growth potentials for specific plant parts. Soils are defined by their water retention and conductivity characteristics, bulk density, pH, and initial conditions for water, inorganic nitrogen, and organic carbon. Daily inputs for minimum and maximum temperature, dew point temperature, solar radiation, wind run, and precipitation are also required. The model simulates plant stress effects from deficit and excess water conditions and from deficit nitrogen conditions, which feed back on the daily plant growth simulation.

The one–dimensional soil water balance module implemented within the CSM is particularly important considering the objectives of this article. The model simulates daily precipitation and irrigation applications as inputs of water to the soil system. Surface runoff is computed using the Natural Resource Conservation Service (NRCS) curve number technique (Chow et al., 1988). After computing runoff, excess precipitation and irrigation water are available for infiltration, pending sufficient storage capacity in the surface soil layer. Otherwise, water is infiltrated until soil saturation is reached, and the remainder is added to the runoff pathway. One–dimensional water flow through the soil layers is computed using a “tipping bucket” approach based on inputs for the lower limit, drained upper limit, and saturated water contents of each soil layer. For soil layers with water contents above the drained upper limit, downward water flux is computed as a fraction of water storage above the drained upper limit, not to exceed the user–specified saturated hydraulic conductivity for the layer. After calculating soil water flow through all the soil layers, water loss to deep seepage is determined based on the downward water flux from the bottom soil layer. A water redistribution algorithm accounts for upward water flux to soil layers with water contents between the lower limit and drained upper limit.

Several methods are available for computing evapotranspiration in the CSM, one of which is based on FAO–56 procedures (Allen et al., 1998). With this method, the model uses the standard FAO–56 equations to compute daily reference ET (ET_0) from the meteorological input data, but the CSM then deviates from FAO–56 methods to determine the actual ET. The main difference is that the crop coefficient (K_c) determined from FAO–56 methods is used to directly compute

actual crop ET from ET_0 , but the model uses K_c to compute potential ET (PET):

$$PET = (K_c)ET_0 \quad (1)$$

The model then partitions PET into potential soil evaporation and potential plant transpiration based on an exponential relationship between PET and simulated LAI. Actual soil evaporation is then computed based on simulated soil water supply, and actual plant transpiration is computed based on soil water supply and the ability of the simulated plant system to extract and transpire water from the soil profile. Since model simulations of actual ET are often less than PET, the K_c used by the model will generally be higher than the K_c used by FAO-56 approaches, which assume that water supplies are always sufficient enough to meet demand. The equation used by the model to determine K_c is:

$$K_c = 1.0 + (EORATIO - 1.0) \cdot \left(\frac{LAI}{6.0} \right) \quad (2)$$

where LAI is the simulated leaf area index of the crop, and EORATIO is a scaling parameter for adjusting the relationship between simulated LAI and K_c . As noted by Tubiello et al. (1999), the model has tended to underestimate potential evapotranspiration for sites in Arizona. This study was the first to incorporate the EORATIO parameter in the CSM-CROPSIM-CERES-Wheat model as a way to adjust potential evapotranspiration rates.

Several methods are available for application of irrigation water in the CSM, the most common of which is to simply apply water according to the dates and amounts specified in the management file. Additional methods allow the model to control irrigation applications, the timing of which is based on a specified threshold for soil water depletion within a specified irrigation management depth. When soil water depletions levels trigger an irrigation event, the model can either apply a specified amount of water or fill the profile to the drained upper limit. Options are also available for applying water based on specified dates and amounts through the last reported day, at which time the model controls irrigation applications through the end of the growing season.

FIELD EXPERIMENTS

As reported by Hunsaker et al. (2007a, 2007b), ET estimation and irrigation scheduling experiments for wheat were conducted at the University of Arizona's Maricopa Agricultural Center (MAC) near Maricopa, Arizona (33.067547° N, 111.97146° W) during the winters of 2003–2004 and 2004–2005. The soil type at the site was a Casa Grande sandy loam, classified as fine-loamy, mixed, hyperthermic, Typic Natrargids. The original objective for research at the site was to determine whether vegetation indices computed from canopy spectral reflectance measurements could be used to estimate basal crop coefficients (K_{cb}) required to compute crop ET and to schedule irrigations using FAO-56 methods (Allen et al., 1998). For both wheat experiments, the field layout consisted of 32 experimental plots, each 11.2 × 21 m and hydrologically isolated with border dikes. The main treatment consisted of two approaches for estimation of basal crop coefficients, one using a “standard” crop coefficient curve (F) as a function of days after emergence and the other using a season-specific crop coefficient curve (N) based on remote

Table 1. Summary of subtreatments for the 2003–2004 and 2004–2005 FAO-56 irrigation scheduling experiments (FISE) for wheat.

Subtreatment Abbreviation	Experimental Variables			No. of Replicates
	K_{cb} Method	Plant Density	Nitrogen Level	
FSH	FAO (F)	Sparse (S)	High (H)	2
FSL	FAO (F)	Sparse (S)	Low (L)	2
FTH	FAO (F)	Typical (T)	High (H)	4
FTL	FAO (F)	Typical (T)	Low (L)	4
FDH	FAO (F)	Dense (D)	High (H)	2
FDL	FAO (F)	Dense (D)	Low (L)	2
NSH	NDVI (N)	Sparse (S)	High (H)	2
NSL	NDVI (N)	Sparse (S)	Low (L)	2
NTH	NDVI (N)	Typical (T)	High (H)	4
NTL	NDVI (N)	Typical (T)	Low (L)	4
NDH	NDVI (N)	Dense (D)	High (H)	2
NDL	NDVI (N)	Dense (D)	Low (L)	2

sensing estimates of LAI from normalized difference vegetation indices (NDVI). Subtreatments of plant density and nitrogen application rate were equally replicated within each main treatment to provide a range of crop growth and water use conditions (table 1). Three plant density levels, designated as sparse (S; ~75 plant m⁻²), typical (T; ~150 plants m⁻²), and dense (D; ~300 plants m⁻²), were used. Nitrogen fertilizer was injected into irrigation pipes at two rates, giving seasonal nitrogen applications of ~80 kg N ha⁻¹ for the low (L) treatment and ~215 kg N ha⁻¹ for the high (H) treatment. A complete random design with incomplete blocks was used.

Hard red spring wheat (*Triticum aestivum* L., cv. Yecora Rojo) was planted at a 0.20 m row spacing on 10–12 December 2003 and on 22 December 2004. To measure soil water contents, neutron access tubes were installed to a depth of 300 cm in the center of each treatment plot, and a 30 cm time-domain reflectometry (TDR) probe was placed 50 cm from each neutron tube. Irrigation border dikes were then formed around each treatment plot. Two gated pipe irrigation lines were installed to flood irrigate individual treatment plots, and irrigation volumes were measured using an in-line, propeller-type flow meter at the inlet of each pipe. Irrigation scheduling procedures based on the two scheduling approaches were initiated in early February for both seasons. Irrigations were scheduled for the day after soil water balance calculations demonstrated 45% depletion from total available root zone soil water. Applied irrigation amounts were 110% of depleted root zone soil water, where the extra 10% was to account for inefficiencies in the irrigation system. Since irrigation schedules for all treatments managed using the standard FAO-56 method were identical (table 2) while that for the NDVI treatments differed among treatment plots, the current simulation study focuses only on the results for standard FAO-56 treatments.

Nitrogen fertilizer was applied to each treatment plot by injecting 32% liquid urea ammonium nitrate into the gated pipe irrigation system (table 2). Calibrated injector pumps were installed near the inlet of the gated pipe to meter the fertilizer into the irrigation water. Abnormally high precipitation levels in January and February 2005 (table 3) complicated nitrogen management for the second wheat experiment. At the recommended time for the first in-season nitrogen application (five-leaf stage), the water contents in the soil were too high to accept irrigation water. The first post-plant fertilization was therefore delayed until early March

Table 2. Irrigation and nitrogen fertilizer management schedules for standard FAO-56 treatments during the 2003-2004 and 2004-2005 irrigation scheduling experiments.

Date	DAP ^[a] (d)	Irrigation (mm)	Fertilizer (kg N ha ⁻¹)	
			Low	High
2003-2004 Experiment				
8 Dec. 2003	-3	--	36.0	36.0
19 Dec. 2003	8	66	--	--
31 Dec. 2003	20	48	--	--
6 Feb. 2004	57	51	--	56.0
4 Mar. 2004	84	57	28.0	56.0
19 Mar. 2004	99	80	28.0	56.0
31 Mar. 2004	111	94	18.5	37.0
16 Apr. 2004	127	86	--	--
26 Apr. 2004	137	80	--	--
Total		562	110.5	241
2004-2005 Experiment				
21 Dec. 2004	-1	--	37.0	37.0
30 Dec. 2004	8	53	--	--
3 Mar. 2005	71	40	--	56.0
22 Mar. 2005	90	80	37.5	75.0
5 Apr. 2005	104	98	28.0	56.0
19 Apr. 2005	118	103	18.5	37.0
2 May 2005	131	89	--	--
Total		463	121.0	261.0

[a] DAP = days after planting.

(table 2), and all subsequent fertilizations were much later in relation to crop development stage than in the first experiment. Delayed fertilizer applications in combination with nitrogen leaching due to heavy rains substantially altered the course of the 2004-2005 experiment with notable reductions in wheat growth and yield. This made the measured dataset especially useful for testing crop water management tools that account for in-season variability in crop growth, such as the Hunsaker et al. (2007a) NDVI approach and the present crop systems modeling approach. Further details on the experimental protocol can be obtained from Hunsaker et al. (2007a, 2007b).

FIELD MEASUREMENTS

Volumetric soil water contents were measured frequently at the center of each treatment plot. Neutron probes (model 503, Campbell Pacific Nuclear, Martinez, Cal.) were used to measure the soil moisture profile from 30 to 290 cm in 20 cm increments, and TDR probes (Trase1, Soil-Moisture Equipment Corp., Santa Barbara, Cal.) were used to measure soil

moisture from the surface to a depth of 30 cm. Initial soil moisture conditions in each treatment plot were measured prior to the first irrigation of each experiment. Thereafter, soil moisture measurements were collected at least weekly and always one day before and three to four days after an irrigation. These data were used in a soil water balance equation (Hunsaker et al., 2005) to generate a "measured" dataset for the deep seepage and ET that occurred between soil moisture measurement dates. Since model simulations were conducted to a depth of 210 cm in this study, neutron probe measurements from 210 cm to 290 cm were used to obtain an estimate of deep seepage. Actual ET was then computed by subtracting deep seepage from the total precipitation, irrigation, and change in soil water storage between soil moisture measurement dates.

Throughout each experiment, extensive agronomic measurements were collected to document wheat growth, development, and yield in each plot. After wheat establishment, plant density measurements were collected to verify acceptability of the three density treatments. Phenology was documented weekly using the Zadoks scale (Zadoks et al., 1974), and canopy height was also measured. Every two weeks following emergence, destructive plant sampling was used to measure various aspects of wheat growth, including above-ground biomass, leaf number, leaf mass, stem mass, spike mass, chaff mass, and grain mass. The green leaf area of dissected plant samples was measured using an area meter (model 3100, Li-Cor, Lincoln, Neb.), and green leaf area index was computed based on leaf area and plant density at emergence. On 26 May 2004 and 27 May 2005, a Hege plot combine (Wintersteiger AG, Ried im Innkreis, Austria) equipped with a 1.5 m cutter bar was used to harvest grain from a 24 m² sample area delineated in the southern portion of each treatment plot.

Studies to characterize the physical and chemical properties of the soil at the field site have been carried out several times. Prior to the 2004-2005 experiment, inorganic nutrient contents of select treatment plots were determined by sending several soil samples to a commercial soil analysis laboratory. In 2005, soil samples were collected at 16 random locations across the field area and analyzed to obtain bulk density. In the spring of 2008, GPS navigation was used to collect soil samples at the original location of the 32 neutron access tubes. Laboratory analysis of these samples provided soil texture information for characterizing soil water retention and conductivity parameters.

Table 3. Monthly summary of meteorological data collected during the 2003-2004 and 2004-2005 irrigation scheduling experiments at Maricopa, Arizona.^[a]

Month	2003-2004 Experiment						2004-2005 Experiment					
	SRAD (MJ m ⁻²)	TMAX (°C)	TMIN (°C)	RAIN (mm)	DEWP (°C)	WIND (km d ⁻¹)	SRAD (MJ m ⁻²)	TMAX (°C)	TMIN (°C)	RAIN (mm)	DEWP (°C)	WIND (km d ⁻¹)
Dec.	358	19.7	1.1	4	-0.3	139	306	18.5	2.5	18	2.6	135
Jan.	346	19.6	3.7	18	3.5	136	320	19.0	5.2	70	7.1	136
Feb.	440	18.9	2.2	23	0.3	146	337	19.5	7.0	86	8.1	152
Mar.	618	29.0	10.4	7	7.3	174	604	23.1	7.3	10	4.8	176
Apr.	755	28.9	11.1	25	3.1	212	774	29.4	9.4	3	0.7	201
May	913	35.9	15.7	0	0.7	205	890	35.2	16.0	0	4.0	191
Sum	3430	--	--	77	--	--	3231	--	--	187	--	--
Mean	--	25.3	7.4	--	2.4	169	--	24.1	7.9	--	4.6	165

[a] SRAD = total incoming solar radiation, TMAX = average maximum daily temperature, TMIN = average minimum daily temperature, RAIN = total precipitation, DEWP = average dew point temperature, and WIND = average daily wind run.

Meteorological data were collected from an Arizona Meteorological Network (AZMET, <http://cals.arizona.edu/azmet/>) station located approximately 100 m north of the study area. The station included a thermistor, a capacitive relative humidity probe, an anemometer, and a pyranometer mounted above a uniform, well-watered grass for determining ambient air temperature, dew point temperature, wind speed, and incoming solar radiation. Precipitation was measured using a tipping-bucket rain gauge. Data from the station were sampled at 10 min intervals throughout each growing season. On an hourly basis, data were aggregated and logged. Daily totals for solar radiation, wind run, precipitation, and maximum and minimum daily temperatures were computed at midnight each evening. Table 3 summarizes the monthly AZMET data in each growing season.

MODEL PARAMETERIZATION

Model parameterization included specification of some model parameters using appropriate field measurements and calibration of more uncertain parameters to improve comparisons of model output and measured data. Model calibration was performed using measurements from the 2004–2005 wheat experiment only. Since nitrogen management decisions were affected by precipitation patterns in this season, we expected the 2004–2005 data to be more useful for model parameterization under nitrogen-limited conditions. Data from the 2003–2004 experiment were used for independent model testing. In relation to 2004–2005, precipitation patterns and nitrogen management for the 2003–2004 season were more typical for wheat in central Arizona. Based on the precipitation differences between the two seasons (table 3) and its affect on nitrogen management (table 2), the two growing seasons were adequately different and useful for testing the model response to interactions of management and climatic variability at this site.

The criteria used to evaluate the model were both objective and subjective in nature. Graphical comparison of measured and simulated data was useful for locating anomalies in the simulated data and to visualize the overall performance of the model. Measured and simulated data were also compared quantitatively by computing several model evaluation statistics (Loague and Green, 1991), but analysis focused primarily on the relative root mean squared error (RRMSE) and the Nash and Sutcliffe (1970) model efficiency (EFF). A Python script was written to automate model simulations, compute error statistics, and plot measured versus simulated data.

Management

The CSM-CROPSIM-CERES-Wheat model was set to simulate the conditions for each of the six standard FAO-56 treatments (FSH, FSL, FTH, FTL, FDH, and FDL). Treatments based on NDVI were not simulated since individual plots could in fact receive different irrigation schedules. Simulations were initiated seven days before planting for both seasons. The model was set to simulate water-limited and nitrogen-limited production with all management, weather, and initial conditions occurring on reported dates. The simulated soil profile was divided into ten layers at depths of 5, 15, 30, 45, 60, 90, 120, 150, 180, and 210 cm from the soil surface. Initial conditions for soil moisture were specified using the neutron and TDR probe readings from the first measurement date of each experiment. Water contents were not ex-

pected to change much between the simulation start dates and the first soil moisture measurement date since water contents were near the lower limit and no precipitation occurred during that time. Initial soil nutrient conditions were not thoroughly characterized, so the initial nitrate concentration in all soil layers and for all treatments was set uniformly to 4.5 g Mg⁻¹ for both seasons based on the soil analysis performed prior to the 2004–2005 season. Initial ammonium concentrations in all soil layers were adjusted to 0.3 g Mg⁻¹, which provided stable ammonium concentration simulations throughout each growing season. Crop planting was simulated on the reported dates with plant density based on measurements collected around the time of emergence. Irrigation applications were simulated with reported dates and amounts given by standard FAO-56 approaches during each field experiment (table 2). Considering the possibility of lateral water percolation into the border dikes and surrounding plot areas, the irrigation efficiency parameter was adjusted to 96% to improve water balance simulations. It is important to note that the irrigation efficiency parameter simply reduces applied irrigation amounts, and the “lost” water is not considered as part of the model’s water balance. Applications of fertilizer were also simulated with reported dates and amounts for each treatment. An incorporation depth of 10 cm was assumed. Crop growth simulations ended on the reported harvest dates for each season.

Meteorology

Weather input files were created from daily meteorological data collected with the AZMET station at the MAC farm. Additional information from the AZMET station was used to set the average soil temperature parameter (TAV) to 22.0 °C and the soil temperature amplitude parameter (AMP) also to 22.0 °C.

Crop Component

Adjustment of the model’s crop development simulation focused on several parameters that govern the progression of the simulation through a series of development stages (table 4). The length of the model’s germination stage is controlled by the PEG parameter, which defines the hydrothermal units (°C d cm cm⁻¹; thermal units multiplied by available soil water in the seed layer) that must accumulate before germination is simulated. The PEG parameter was adjusted to 75 °C d cm cm⁻¹ such that germination was simulated one day after the first irrigation event in each season. The length of the emergence stage is controlled with the PECM parameter, which defines the thermal units per unit seed depth (°C d cm⁻¹) that must accumulate before emergence is simulated. The PECM parameter was adjusted to 35 °C d cm⁻¹ such that emergence was simulated on the observed date of 50% plant emergence. The model’s P1 stage defines the duration from emergence to double ridges, the stage at which distinct leaf and spikelet primordia are distinguishable. The number of thermal units required to complete the P1 stage is defined by the P1 parameter, but daily accumulation of thermal units in this stage can be reduced based on the P1V and P1D parameters, which control vernalization and photoperiod sensitivity, respectively. To adjust the simulation of the P1 stage, the P1 parameter was first set to a reasonable value of 400 °C d. The P1V parameter, which defines the days at optimum vernalizing temperature required to complete vernalization, was then set to 5 d. This is the same value used by Tubiello et al. (1999) when adjusting by a fac-

tor of 10 to account for coding differences between the current model version and the one used previously. Since planting dates were similar in both growing seasons, we do not have good data to understand the sensitivity of the Yecora Rojo wheat variety to day length. Pinter et al. (2000) notes the variety to be photoperiod insensitive. Our strategy was to adjust the P1D parameter, which controls the rate of development in relation to photoperiod in the P1 stage, to improve simulations of Zadoks number. The final calibrated value for P1D was 12%, a relatively low value that indicates photoperiod insensitivity. The model's P2 stage defines the duration from the double ridge phase to the end of leaf growth. The number of thermal units required to progress through the P2 stage was adjusted to 350 °C d to improve Zadoks number simulations. Since the end of the P2 stage is marked by the cessation of leaf growth, time series plots of measured and simulated leaf mass and LAI were also helpful to determine the approximate date for the end of the P2 stage. During the P1 and P2 vegetative development stages, the PHINT parameter controls the rate of leaf number development. We adjusted PHINT to 105 °C d to improve simulations of leaf number as compared to laboratory leaf number measurements from biomass samples and to ensure that the model simulated a maximum of eight leaves in each season, which is typical for Yecora Rojo. The TI1LF parameter, adjusted to 1.5 leaves, defines the leaf number at which tillering begins and was useful for improving simulations of Zadoks number in the P1 and P2 stages. The model simulates reproductive development in three stages, P3, P4, and P5, which define the durations of the spike growth period, the grain fill lag period, and the linear grain filling period. Thermal units required to progress through these three development stages were adjusted to 150, 400, and 430 °C d, respectively, to improve Zadoks number simulations. The model simulates the onset of anthesis when one quarter of the required thermal units for the P4 stage are accumulated, and physiological maturity is simulated at the end of the P5 stage. For all crop development calculations, the model computes growing degree day accumulation using a base temperature of 0 °C.

After finalizing the crop development simulation, calibration efforts focused on adjustment of the model's biomass growth simulation. The PARUV and PARUR parameters control the conversion of photosynthetically active radiation (PAR) to dry matter during the P1 and P2 vegetative development stages and the P3, P4, and P5 reproductive development stages, respectively. To improve time series simulations of aboveground biomass as compared to measurements, PARUV was adjusted to 2.2 g MJ⁻¹ and PARUR was adjusted to 2.4 g MJ⁻¹ (table 4). During the P1 and P2 stages, the model partitions biomass mainly to leaves, with increasing partitioning to stems as the simulation progresses through vegetative development. Leaf growth is simulated in two phases during this period, where the LAVS and LARS parameters define the potential area of leaves in the first and second phases, respectively. To improve simulations of leaf mass as compared to measurements, LAVS was adjusted to 25 cm² and LARS was adjusted to 50 cm². Accurate simulation of LAI is particularly important, since the LAI state variable is used in the computation of both PAR interception and potential evapotranspiration (eq. 2). The LAWRS and LAWR2 parameters govern the relationship between laminar leaf area and leaf mass for the first and second leaf phases, respectively. To improve simulations of LAI as compared to measure-

Table 4. Important model parameters that control crop development, growth, and yield simulations.

Parameter	Description	Value
Crop Development		
PEG	Duration of phase from planting to germination (°C d cm cm ⁻¹) ^[a]	75
PECM	Duration of phase from germination to emergence (°C d cm ⁻¹) ^[a]	35
P1	Duration of phase from emergence to double ridges (°C d) ^[b]	400
P1D	Percentage reduction in development rate in a photoperiod 10 hour shorter than the threshold relative to that at the threshold ^[a]	12
P1V	Days at optimum vernalizing temperature required to complete vernalization ^[c]	5
P2	Duration of phase from double ridges to the end of leaf growth (°C d) ^[a]	350
P3	Duration of phase from the end of leaf growth to the end of spike growth (°C d) ^[a]	150
P4	Duration of phase from the end of spike growth to the end of the grain fill lag (°C d) ^[a]	400
P5	Duration of the grain filling phase (°C d) ^[a]	430
PHINT	Interval between successive leaf tip appearances (°C d) ^[a]	105
TI1LF	Leaf number at which tillering begins ^[a]	1.5
Crop Growth		
PARUV	Conversion rate from photosynthetically active radiation to dry matter before the end of leaf growth (g MJ ⁻¹) ^[a]	2.2
PARUR	Conversion rate from photosynthetically active radiation to dry matter ratio after the end of leaf growth (g MJ ⁻¹) ^[a]	2.4
LAVS	Potential area of first phase leaves (cm ²) ^[a]	25
LARS	Potential area of second phase leaves (cm ²) ^[a]	50
LAWRS	Laminar area to weight ratio of first phase leaves (cm ² g ⁻¹) ^[b]	250
LAWR2	Laminar area to weight ratio of second phase leaves (cm ² g ⁻¹) ^[b]	230
Crop Yield		
G1	Kernel number per unit canopy weight at anthesis (kernels g ⁻¹) ^[a]	20
G2	Standard kernel size under optimum conditions (mg) ^[a]	54
G3	Standard, non-stressed dry weight of a single tiller at maturity (g) ^[b]	1.5
RSFRS	Fraction of carbon assimilates partitioned to reserves prior to the end of stem growth ^[a]	0.12
GRNMN	Minimum grain nitrogen concentration (%) ^[a]	2.0
GRNS	Standard grain nitrogen concentration (%) ^[a]	3.0

^[a] Parameter adjusted to improve measured vs. simulated relationships.

^[b] Parameter value selected from a subset of default values.

^[c] Parameter value based on the results of Tubiello et al. (1999).

ments, LAWRS was set to 250 cm² g⁻¹, while LAWR2 was set to 230 cm² g⁻¹. These values were chosen based on a subset of default values provided in the files distributed with the model.

Wheat yield simulations are influenced by several parameters that control kernel set, potential grain size, reserves mass accumulation, and nitrogen concentration in grain. Measurements were available to describe the average weight of individual wheat kernels, so the G2 parameter, which defines the potential kernel size, was adjusted to 54 mg such that

simulated kernel weight was reasonable with respect to the measurements (table 4). The G3 parameter defines the standard dry weight of a single tiller at maturity, but G3 was not shown to substantially affect crop yield simulations. A default value of 1.5 g was used for G3. Remaining parameters were adjusted to minimize RRMSE between measured and simulated wheat yield. The G1 parameter controls the kernel number per unit canopy weight at anthesis and was adjusted to 20 kernels g⁻¹. A critical adjustment involved the RSFRS parameter, which controls the fraction of carbon assimilates partitioned to reserves before the end of stem growth. RSFRS was adjusted to a value of 0.12 to improve wheat yield simulations as well as the carbon allocation to leaves and stems in the reproductive development stages. Finally, due to the nitrogen stress effects that resulted from abnormally high precipitation in 2004–2005, adjustment of the grain nitrogen concentration parameters was needed to improve yield simulations in that season. The parameters for minimum grain nitrogen concentration (GRNMN) and the standard grain nitrogen concentration (GRNS) were adjusted to values of 2.0% and 3.0%, respectively, to improve simulations of grain yield and final grain N concentration with respect to measurements.

Equation 2 demonstrates one aspect of the interaction between the crop growth component and the water balance component of the model for the ET method used in these simulations. After appropriately adjusting the crop parameters as described above, the EORATIO parameter was adjusted to a value of 1.8 to provide crop coefficient (K_c) values that improved simulations of actual ET at the site.

Soil Component

Simulations were performed using one set of average soil conditions for the site (table 5). Model inputs for silt content (SLSI) and clay content (SLCL) were based on the average of soil texture measurements collected within each standard FAO-56 plot in 2008. Soil bulk density values (SBDM) were based on the average of the 16 random bulk density measurements across the field in 2005. The ROSETTA pedotransfer functions (Schaap et al., 2001) were used to calculate the lower limit (SLLL), drained upper limit (SDUL), saturated soil water content (SSAT), and saturated hydraulic conductivity (SSKS) for each soil layer, based on soil texture measurements from each of the standard FAO-56 plots. The drained upper limit in each soil layer was then adjusted within 0.03 cm cm⁻¹ of the average ROSETTA value to improve

simulations of soil water contents in each soil layer. Soil root growth factors (SRGF) were specified by analyzing neutron probe data to understand how water was taken up along the depth of the profile. With root growth factors in the top 30 cm set equal to 1.0, the factors below 30 cm were based on an exponential decay function with depth. Initial soil organic carbon (SLOC) and electrical conductivity (SCEC) were based on the MAC farm soil descriptions of Post et al. (1988). Soil pH in water (SLHW) was obtained from a digital soil survey of the site. In addition to the parameters specified by depth, the drainage rate (SLDR) was adjusted to a value of 0.14 d⁻¹ to reduce error between measured and simulated soil water contents, and the runoff curve number (SLRO) was adjusted to a very low value of 1.0 to force the model to simulate zero runoff. We expected no runoff from diked treatment plots.

MODEL APPLICATION

For many applications of crop systems models, such as analysis of water management alternatives, development of irrigation schedules, or assessment of regional water demands, knowledge of specific irrigation management inputs are largely unknown. In fact, the point of these applications is often to gain insight from the model on better ways to manage water. However, before the model's decision making skills can be trusted, it must be shown that its automatic irrigation algorithms can provide reasonable irrigation schedules. To address this issue, further simulation studies were conducted to evaluate the ability of the model's automatic irrigation routine to reproduce the FAO-56 irrigation schedules devised during field experimentation. The first two irrigations for the 2003–2004 experiment and the first irrigation for the 2004–2005 experiment, which were applied to initiate germination, were simulated as applied for both seasons (table 2). After these initial irrigations, the model was set to conduct automatic irrigations for the remainder of the growing season. Using data from the neutron probes to estimate the actual depth of root water uptake, the model's irrigation management depth parameter was set to 65 cm. Similar to the actual experiments, the model was set to initiate irrigations when soil water contents within the management depth reached 45% depletion from total available water. Irrigation volumes refilled the profile to the drained upper limit, which was the maximum allowed by the model. Finally, the calibrated irrigation efficiency of 96% was used. As discussed in the results, several deficiencies in model design were noted while setting up automatic irrigations.

Table 5. Soil parameters used as model input for all simulated treatments.^[a]

Depth (cm)	SLLL (cm cm ⁻¹)	SDUL (cm cm ⁻¹)	SSAT (cm cm ⁻¹)	SRGF (-)	SSKS (cm h ⁻¹)	SBDM (g cm ⁻³)	SLOC (%)	SLCL (%)	SLSI (%)	SLHW (-)	SCEC (cmol kg ⁻¹)
0-5	0.093	0.226	0.407	1.000	1.5	1.49	0.58	21.0	10.8	8.3	12.0
5-15	0.093	0.226	0.407	1.000	1.5	1.49	0.58	21.0	10.8	8.3	12.0
15-30	0.093	0.226	0.407	1.000	1.5	1.49	0.58	21.0	10.8	8.3	12.0
30-45	0.099	0.228	0.435	0.657	2.0	1.40	0.17	22.6	10.8	8.3	12.0
45-60	0.103	0.249	0.431	0.432	1.9	1.42	0.17	24.1	10.7	8.3	12.0
60-90	0.106	0.251	0.399	0.186	1.2	1.53	0.17	24.0	12.5	8.3	12.0
90-120	0.098	0.247	0.382	0.080	1.0	1.58	0.17	21.4	11.8	8.3	12.0
120-150	0.078	0.234	0.377	0.035	1.7	1.58	0.17	16.9	9.2	8.3	12.0
150-180	0.088	0.221	0.380	0.015	1.3	1.58	0.17	19.2	9.4	8.3	12.0
180-210	0.088	0.251	0.380	0.006	1.3	1.58	0.17	19.2	9.4	8.3	12.0

^[a] SLLL = lower limit, SDUL = drained upper limit, SSAT = saturated soil water content, SRGF = soil root growth factor, SSKS = saturated hydraulic conductivity, SBDM = bulk density, SLOC = organic carbon content, SLCL = clay content, SLSI = silt content, SLHW = pH in water, and SCEC = cation exchange capacity.

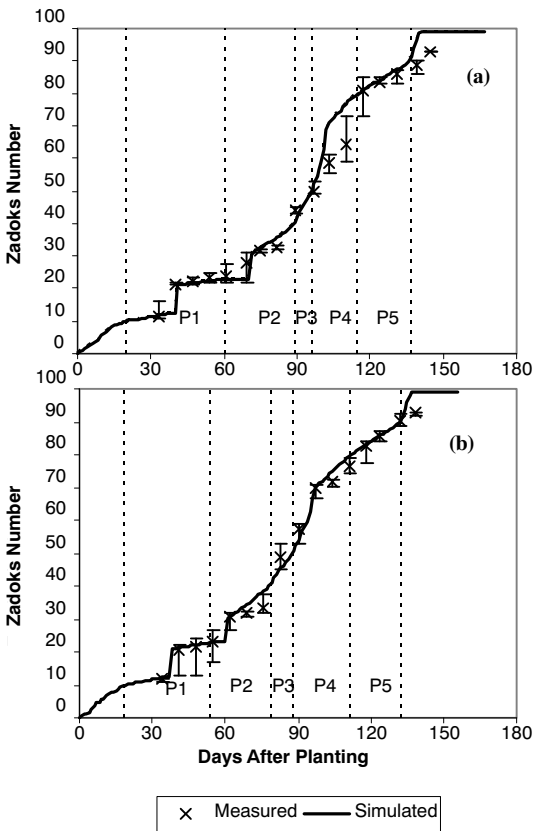


Figure 1. Average measured and simulated Zadoks number for standard FAO-56 treatments in the (a) 2003-2004 and (b) 2004-2005 FISE wheat experiments. Error bars demonstrate the maximum and minimum of the Zadoks scale measurements. Progression of the simulated crop development stages from emergence (beginning of P1) through physiological maturity (end of P5) are noted.

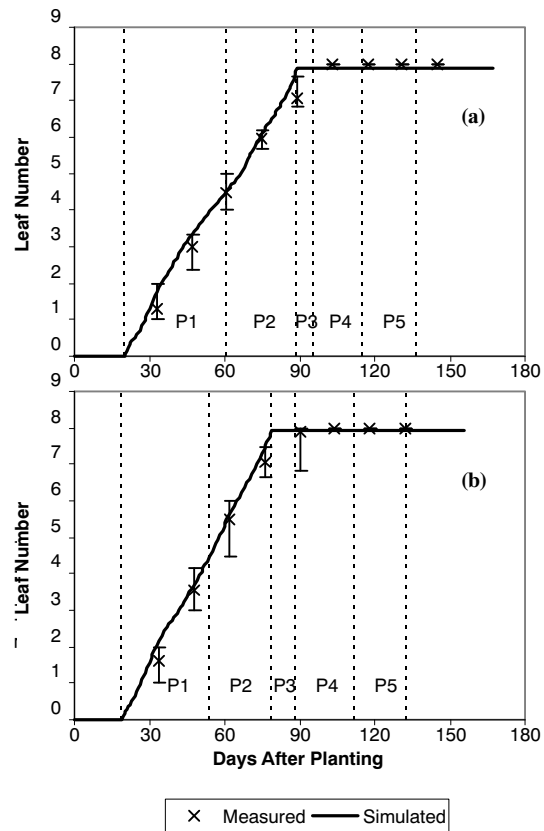


Figure 2. Average measured and simulated leaf number for standard FAO-56 treatments in the (a) 2003-2004 and (b) 2004-2005 FISE wheat experiments. Error bars demonstrate the maximum and minimum of the leaf number measurements. Progression of the simulated crop development stages from emergence (beginning of P1) through physiological maturity (end of P5) are noted.

RESULTS AND DISCUSSION

CROP COMPONENT SIMULATION

Crop Development

Adjustment of the 11 parameters that influence crop development (table 4) resulted in favorable simulations of Zadoks number as compared to measurements in both seasons (fig. 1). Among the simulations for the six standard FAO-56 treatments, simulated Zadoks number on a particular day did not differ by more than 0.02 from the mean value, so the average simulated Zadoks number is sufficient to demonstrate the model response. Variability in measured Zadoks number is demonstrated using error bars to represent the maximum and minimum number collected on each measurement date. Progression of the model simulations through the five development stages from emergence to physiological maturity, P1 through P5, is also shown in figure 1. The simulations demonstrated that crop development proceeded more quickly in the 2004-2005 season as compared to the 2003-2004 season. For both seasons, the model reasonably simulated the date of crop emergence. For the 2004-2005 season, crop emergence was simulated 19 days after planting (DAP) for all standard FAO-56 treatments, and 50% crop emergence was also measured 19 DAP. For the 2003-2004 season, 50% crop emergence was measured 19 DAP, and the model simulated emergence 20 DAP for all treatments. After emergence, the model reasonably simulated the onset of main shoot and tiller growth with jumps to 20 on the Zadoks scale midway through

the P1 development stage. Thereafter, the model simulated Zadoks number reasonably well in both seasons through the completion of booting at the end of P3. Onset of anthesis was simulated 100°C d into the P4 development stage in both seasons, which corresponds to a Zadoks number of 60. Using linear interpolation to compute the DAP for measured Zadoks number equal to 60, the measured anthesis dates among standard FAO-56 treatment plots ranged from 102 to 111 DAP in the 2003-2004 season and from 93 to 95 DAP in the 2004-2005 season. The model simulated anthesis 101 DAP and 95 DAP in the 2003-2004 and 2004-2005 seasons, respectively. Thus, simulations of anthesis were slightly early in 2003-2004, while they were within the measured range for the 2004-2005 season. Temperature differences between the two seasons (table 3) were responsible for the slower crop development rates in 2003-2004. Comparing heat unit accumulation for the two seasons from 19 to 95 DAP, the 2003-2004 season lagged behind the 2004-2005 season by 115°C d . With the exception of a slightly overestimated Zadoks number during P4 in 2003-2004, simulations of Zadoks number in both seasons were reasonable with respect to measurements from anthesis to physiological maturity. Using linear interpolation to compute the DAP for measured Zadoks number equal to 90, the measured dates for physiological maturity among standard FAO-56 treatment plots ranged from 137 to 140 DAP in the 2003-2004 season and from 132 to 136 DAP in the 2004-2005 season. The model simulated an-

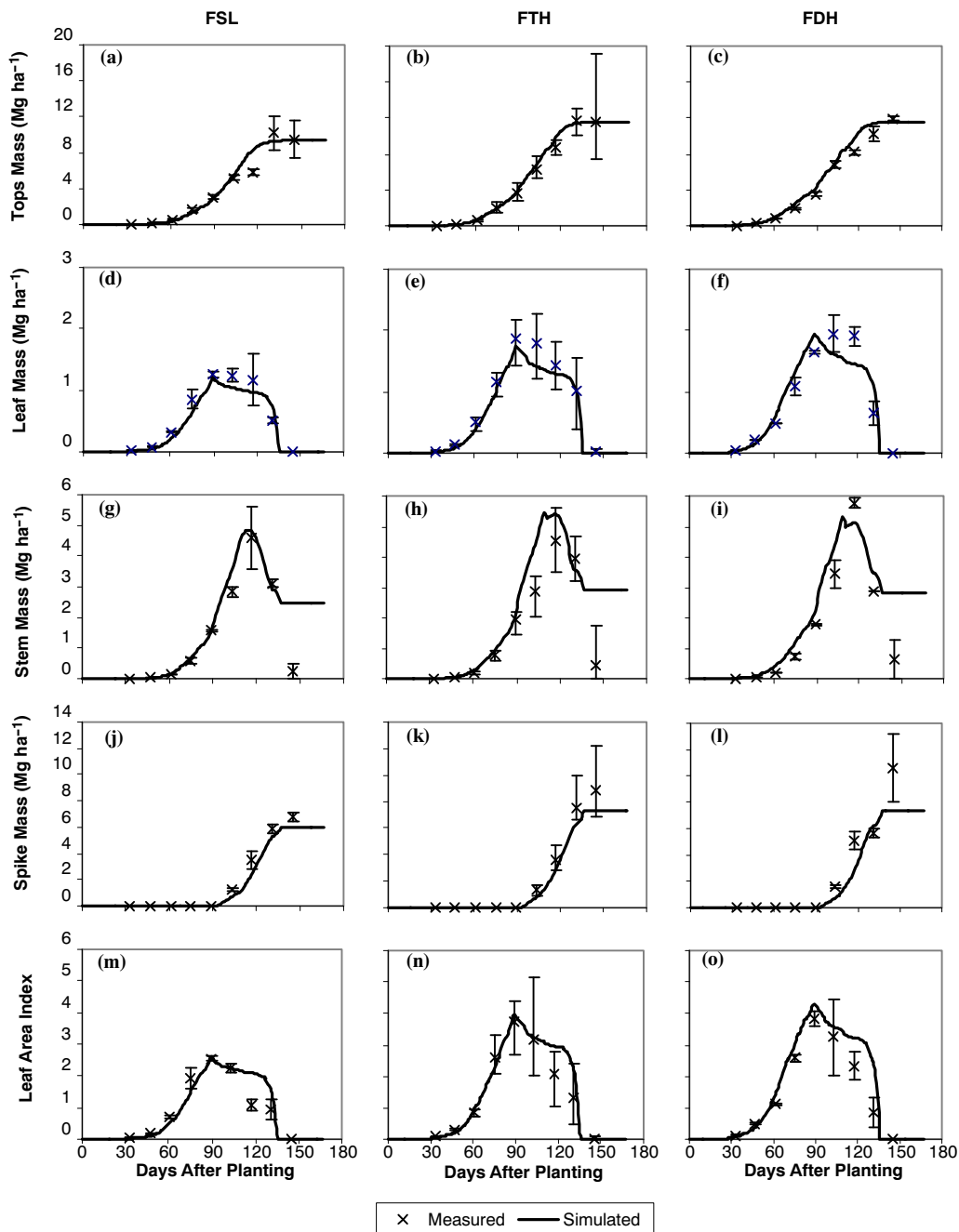


Figure 3. Average measured and simulated crop growth results for (a-c) total aboveground biomass, (d-f) leaf mass, (g-i) stem mass, (j-l) spike mass, and (m-o) leaf area index for the standard FAO-56, sparse population, low nitrogen (FSL) treatment; the standard FAO-56, typical population, high nitrogen (FTH) treatment; and the standard FAO-56, dense population, high nitrogen (FDH) treatment, respectively, during the 2003-2004 FISE wheat experiment. Error bars demonstrate the maximum and minimum of measurements.

thesis 137 DAP and 133 DAP in the 2003-2004 and 2004-2005 seasons, respectively. These results demonstrate that the model can respond appropriately to the effects of seasonal temperature differences on crop development.

The time series of measured and simulated leaf number demonstrated reasonable leaf development simulations in both seasons (fig. 2), indicating appropriate adjustment of the PHINT parameter (table 4). Eight total leaves were developed in the simulations for both seasons, which is typical for the Yecora Rojo wheat variety. Simulations of leaf number did not vary among the six standard FAO-56 treatments. Variability in measured leaf number is demonstrated using

error bars to represent the maximum and minimum leaf number on each measurement date.

Crop Growth

For the 2003-2004 season (fig. 3) and the 2004-2005 season (fig. 4), measured and simulated crop growth results are presented for the FSL, FTH, and FDH treatments. Space restraints limited our ability to show the simulated crop growth responses for all of the treatments, but results for these three treatments demonstrate the model's ability to respond to different plant populations and nitrogen rates. Treatment averages computed from the measured crop growth data on each

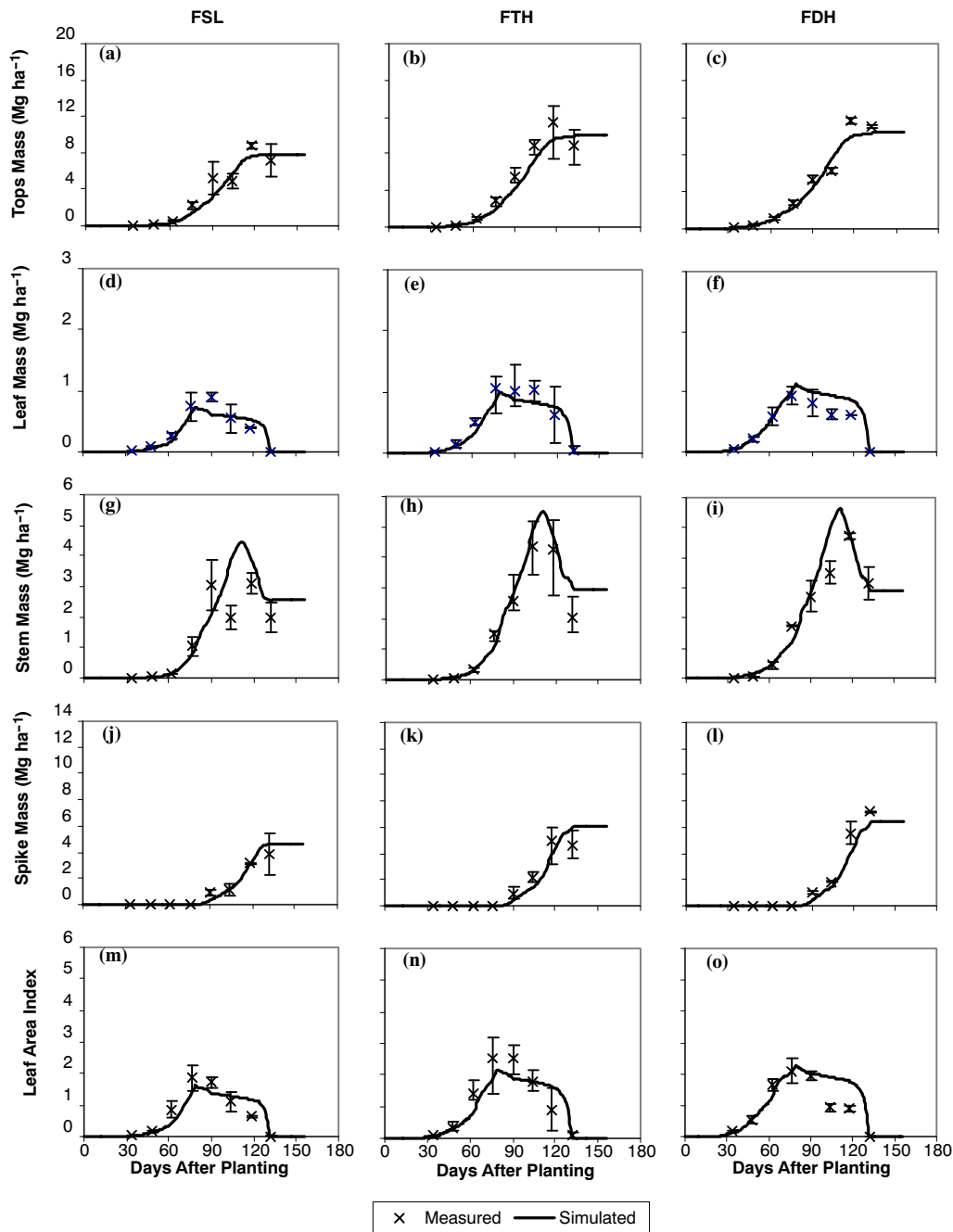


Figure 4. Average measured and simulated crop growth results for (a-c) total aboveground biomass, (d-f) leaf mass, (g-i) stem mass, (j-l) spike mass, and (m-o) leaf area index for the standard FAO-56, sparse population, low nitrogen (FSL) treatment; the standard FAO-56, typical population, high nitrogen (FTH) treatment; and the standard FAO-56, dense population, high nitrogen (FDH) treatment, respectively, during the 2004-2005 FISE wheat experiment. Error bars demonstrate the maximum and minimum of measurements.

biweekly measurement date are plotted in figures 3 and 4, along with error bars representing the maximum and minimum measured value.

The RRMSE between average measured and simulated aboveground biomass on the final measurement dates in each season were 9.5% and 12.1% for 2003-2004 and 2004-2005, respectively, indicating adequate adjustment of the PARUV and PARUR parameters (table 4) that govern the conversion of PAR to biomass. Measurements of leaf mass nearest to the end of leaf development occurred 89 DAP and 76 DAP in 2003-2004 and 2004-2005, respectively. The RRMSE between average measured and simulated leaf mass on these

dates were 12.0% for 2003-2004 and 17.2% for 2004-2005, indicating adequate adjustment of the LAVS and LARS parameters that govern potential leaf size. Similarly, the RRMSE between average measured and simulated LAI on these dates were 17.9% for 2003-2004 and 20.6% for 2004-2005. Higher errors for LAI resulted from the tendency of the model to underestimate LAI for the FSH treatment in both seasons (not shown). Simulations of peak leaf mass and peak LAI for the 2003-2004 season (fig. 3) best demonstrate the ability of the model to respond to differences in plant population and nitrogen application rates. For the FSL, FTH, and FDH treatments in 2003-2004, the model simulated peak leaf

masses of 1.2, 1.7, and 1.9 Mg ha⁻¹, respectively, at 89 DAP. Similarly, peak simulations of LAI were 2.6, 4.0, and 4.3 for the FSL, FTH, and FDH treatments, respectively. Measurements reflected the simulated differences in these variables. A similar response, although less pronounced, is distinguishable among the treatments for the 2004–2005 simulations (fig. 4). For the FSL, FTH, and FDH treatments in 2004–2005, the model simulated peak leaf masses of 0.7, 1.0, and 1.1 Mg ha⁻¹, respectively, at 79 DAP, and peak simulations of LAI were 1.6, 2.2, and 2.3, respectively. These values represent approximately 40% to 45% reductions in simulated leaf mass and LAI as compared to the 2003–2004 season (fig. 3), a result that was also reflected in the measurements. As noted previously, precipitation in January and February of 2005 was above average (table 3), which resulted in leached nitrogen in the early season and delayed fertilizer applications in 2004–2005 (table 2). Nitrogen stress resulting from these conditions caused a marked reduction in plant growth, and the model captures these effects well. Simulations of peak stem mass were not noticeably different between the two growing seasons, although it is clear that the model simulated less stem growth for the FSL treatment in both seasons. As reflected in the measurements, the model simulated more spike growth in 2003–2004 than in 2004–2005, a direct effect of the higher nitrogen stress simulated in the latter season. It is interesting to note that the model consistently overestimates LAI in the late season, approximately 120 DAP (figs. 3 and 4). Based on these results, there is considerable evidence that the model is reasonably responding to differences in meteorological conditions and management practices between and among the two growing seasons.

Crop Yield

Because of the abnormal weather conditions during the 2004–2005 season, measured wheat yields were typically lower during this season as compared to the 2003–2004 season. A scatterplot of simulated versus measured wheat yield demonstrates the ability of the model to respond to treatment variability within a single season as well as management and meteorological differences between the two seasons (fig. 5). Variability in measured yield is demonstrated using error bars to represent the maximum and minimum measurements for each treatment. For the 2003–2004 season, yield simulations among the different treatments were reasonable, with an RRMSE of 7.4% and an EFF of 0.62. The model tended to overestimate yield for the FDL treatment in this season with a simulated value of 5.4 Mg ha⁻¹ while the average measured value was 4.5 Mg ha⁻¹. In addition, the model tended to underestimate yield for the FSH treatment in 2003–2004 with a simulated value of 5.7 Mg ha⁻¹ while the average measured value was 6.2 Mg ha⁻¹. Since these two treatments contrast the dense population and low nitrogen rate with the sparse population and high nitrogen rate, these results may indicate an interaction between plant population and nitrogen rates that the model has trouble simulating in this season. Calibrated yield simulations for the 2004–2005 season were very favorable, with an RRMSE of 1.7% and an EFF of 0.98. Overall, these results demonstrate that the model is adequately simulating the within-season effects of different plant populations and nitrogen rates on wheat yield as well as the yield responses that resulted from weather and management variability between the two seasons.

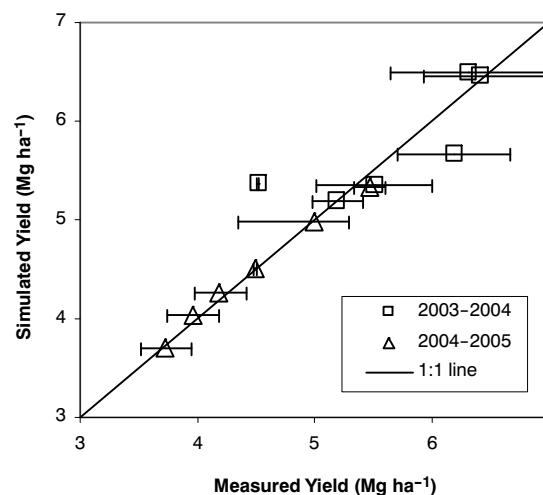


Figure 5. Simulated versus average measured yield for the standard FAO-56 treatments of the 2003–2004 and 2004–2005 FISE wheat experiments. Error bars demonstrate the maximum and minimum of yield measurements.

WATER BALANCE SIMULATION

Soil Water Storage

The time series of measured and simulated soil water contents demonstrate the ability of the model to simulate soil water fluctuations in different soil layers throughout each growing season (figs. 6 and 7). Among the simulations for the six standard FAO-56 treatments, simulated soil water contents were typically within 0.02 cm cm⁻¹ of the mean value, although occasionally the difference was up to 0.06 cm cm⁻¹. For simplicity, we plot only the average simulated soil water content among treatments to demonstrate the model response. Variability in measured soil water content is demonstrated using error bars to represent the maximum and minimum of the neutron probe readings collected within the 16 standard FAO-56 treatment plots on each measurement date. Substantial variability is evident in the measured soil moisture data, which can be attributed to variable crop water use responses to management differences among the treatments (table 1) as well as to differences in the soil water retention characteristics among the treatment plots. Since we have parameterized the model with field-average soil properties (table 5), we expect the model to simulate only the field-average soil moisture conditions. Results suggest that the model is doing an adequate job of this, with RRMSEs between average measured and simulated soil water contents ranging from 8.7% to 18.9% in the layers above 45 cm and from 2.7% to 7.9% in the layers below 45 cm.

For the 2003–2004 season, increases in soil water contents in response to the two early season irrigations, 8 and 20 DAP, are evident in both the measured and simulated data for the top 30 cm of the soil profile (fig. 6). In the lower layers, these early season irrigations served to bring water contents to the drained upper limit until about 70 DAP, when roots began to draw water from the soil layers at the 30–45 and 45–60 cm depths. Approximately 90 DAP, model simulations and measurements indicated that the roots began to draw a relatively small amount of water from the 60–90 cm soil depth. However, no root activity was apparent in either the measured or simulated data for the 90–120 cm soil depth, indicating that water contents at this depth had little effect on water use. Similar to the 90–120 cm soil depth, measured and simulated wa-

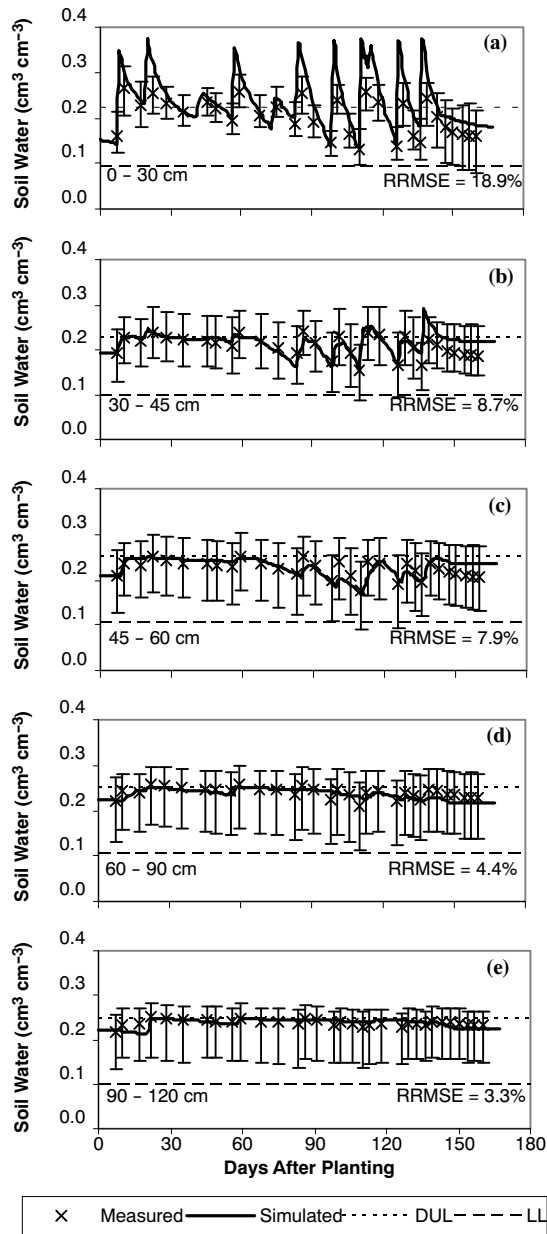


Figure 6. Average measured and simulated soil water contents in soil layers from (a) 0 to 30 cm, (b) 30 to 45 cm, (c) 45 to 60 cm, (d) 60 to 90 cm, and (e) 90 to 120 cm for the 2003-2004 FISE experiment. Error bars demonstrate the maximum and minimum of soil moisture measurements. The drained upper limit (DUL), lower limit (LL), and the relative root mean squared error (RRMSE) for each soil layer are given.

ter contents in the deeper soil layers (not shown) were maintained around the drained upper limit throughout the entire growing season. For some of the treatments, the model had difficulty simulating soil water contents in the late season, from 138 to 168 DAP for the 2003-2004 experiment. A limitation in the model may be the cause for this, since simulated crop transpiration ceased after the simulated day of physiological maturity. In reality, the plant transpiration processes may shut down more gradually over time, as demonstrated by the measurements.

For the 2004-2005 season, evidence of the abnormal precipitation levels in the early season can be seen in the measured and simulated soil water content data (fig. 7). An 11 mm precipitation event 7 DAP followed by 53 mm of ir-

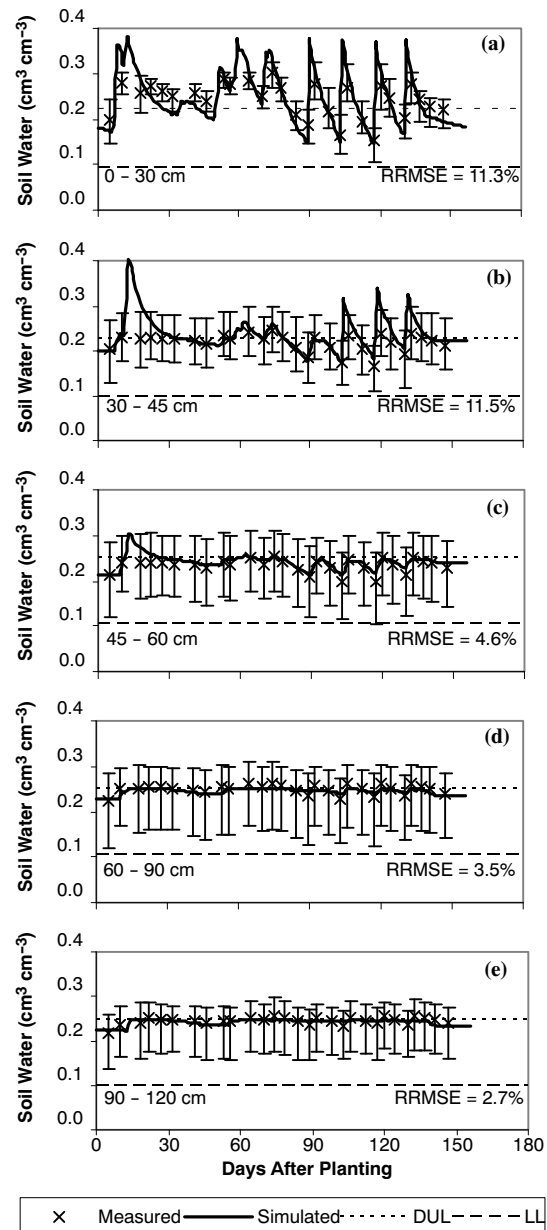


Figure 7. Average measured and simulated soil water contents in soil layers from (a) 0 to 30 cm, (b) 30 to 45 cm, (c) 45 to 60 cm, (d) 60 to 90 cm, and (e) 90 to 120 cm for the 2004-2005 FISE experiment. Error bars demonstrate the maximum and minimum of soil moisture measurements. The drained upper limit (DUL), lower limit (LL), and the relative root mean squared error (RRMSE) for each soil layer are given.

rigation water on the next day initially increased the soil water contents. However, over the next six days, the field was inundated with 57 mm of additional precipitation. As demonstrated in both the measurements and simulations, this event saturated the soil to a depth of 60 cm, a condition that lasted for several weeks. Additional precipitation around 35, 50, and 60 DAP maintained high soil water levels well into the season, which prevented required fertigations until the irrigation event occurring 71 DAP (table 2). Thereafter, both measurements and simulations suggest that substantial root water uptake began to occur to a depth of 60 cm. The effects of no simulated crop transpiration after physiological maturity were not as evident in 2004-2005 as compared to 2003-2004.

ET and Deep Seepage

Since the model was adjusted to simulate no runoff from the diked treatment plots, ET and deep seepage were the only pathways considered for loss of water from the system. Results demonstrated reasonable simulations of ET from emergence to physiological maturity (fig. 8a). Relative root mean squared errors between measured and simulated ET were 2.4% in 2003–2004 and 3.2% for 2004–2005, indicating adequate adjustment of the EORATIO parameter that governs the computation of potential ET. Although these simulations were reasonable, the model did tend to underestimate ET in 2004–2005, while it tended to overestimate ET in 2003–2004. This may be caused by the dependence of the potential ET calculation on simulated LAI (eqs. 1 and 2). Since LAI was generally much lower in 2004–2005 than in 2003–2004 (fig. 3 and 4), equation 2 may be somewhat oversensitive to the effect of LAI on potential ET. Deep seepage from emergence to physiological maturity was simulated reasonably in 2004–2005 (fig. 8b) with an RRMSE of 25.5% between measured and simulated values. However, the model did not simulate any deep seepage for any of the treatments in 2003–2004. Since the magnitude of seepage measurements in 2003–2004, roughly 30 mm, is only 5% of the 639 mm precipitation and irrigation inputs in that year (tables 2 and 3), the seepage volumes for this agricultural system are clearly within the range of expected modeling error. With the measurement error associated with tipping-bucket rain gauges and neutron probes as well as uncertainty in the amount of water lost laterally to berms, it is reasonable to expect that the model could have difficulty simulating deep seepage appropriately. This result must be considered before using the model for crop water management applications that rely on the deep seepage output. Similar issues have been reported with the deep seepage and artificial subsurface drainage simulations of other crop systems models (Eitzinger et al., 2004; Sau et al., 2004). It is also interesting to note that a substantial portion of the measured deep seepage volume can often be accounted for in the error associated with the ET simulation. With average ET of about 500 mm among treatments in 2003–2004 and an RRMSE of 3.2%, error in the ET simulation accounts for roughly 16 mm of water, about half of the measured drainage volume. Error associated with the simulation of soil water storage (fig. 6) accounts for another 25 mm of water in 2003–2004. Since the ET simulation and soil water retention definitions tend to drive the water balance simulations, improvements in these aspects of the model will likely lead to more reliable simulations of deep seepage. Ability of the model to simulate root growth, which is very difficult to validate due to lack of appropriate measurement techniques, may also be related to these water balance issues.

NITROGEN BALANCE SIMULATION

Since the original objective of the field experiments was related to water management, minimal measured information was available to characterize the nitrogen balance at the site. Although we would expect the simulation of no seepage in 2003–2004 (fig. 8b) to affect the simulation of nitrogen leaching, the RRMSE and EFF between measured and simulated nitrogen in harvested grain were 10.9% and 0.16, respectively, indicating reasonable model simulations. However, for the 2004–2005 season, the RRMSE and EFF between measured and simulated nitrogen in harvested grain

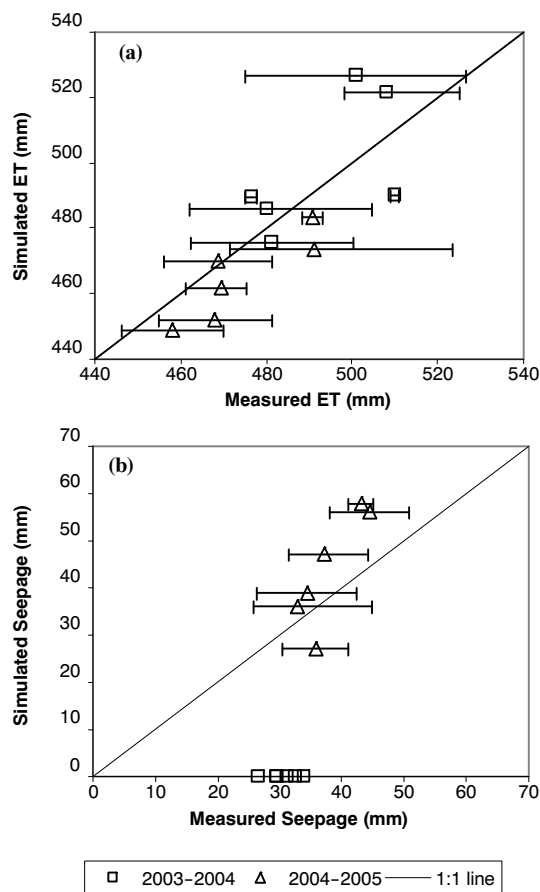


Figure 8. Average measured versus simulated (a) evapotranspiration (ET) and (b) deep seepage from emergence to physiological maturity for the standard FAO-56 treatments of the 2003–2004 and 2004–2005 FISE wheat experiments. Error bars demonstrate the maximum and minimum of the ET and deep seepage estimates from neutron probe data.

were 29.8% and -15.8, respectively, and the grain nitrogen simulation for all treatments were basically level at the 2.0% minimum grain nitrogen concentration (table 4) while measurements averaged 2.8%. This result may be related to the nitrogen stress effects in 2003–2004 due to late mid-season applications of nitrogen fertilizer (table 2). Without further measured information to characterize the nitrogen balance at this site, there is little more that can be done to evaluate the model's nitrogen balance simulations, although results of the study have demonstrated that the model's crop growth and yield simulations are responding appropriately to variable nitrogen rates (figs. 3, 4, and 5).

AUTOMATIC IRRIGATIONS

Several deficiencies in the design of the model's automatic irrigation component prevented the model from computing water requirements similar to the FAO-56 irrigation schedule (fig. 9). After the two irrigation events to initiate germination in 2003–2004, FAO-56 approaches called for irrigation 57 DAP, while the model did not call for irrigation until 85 DAP for the FTH treatment. Similarly, in 2004–2005, FAO-56 approaches called for the first irrigation event 71 DAP, while the model did not call for irrigation until 87 DAP for the FTH treatments. Simulations for other treatments (not shown) provided similar delayed irrigations in the early season. The reason for this result is related to the speci-

fication of a single management depth for automatic irrigations. If the irrigation management depth parameter is estimated from maximum root depth, then early season irrigations will be scheduled late because at that time roots are only drawing water from the top soil layer while deeper soil layers remain filled to the drained upper limit (figs. 6 and 7). This affects the computation of soil water depletion within the management depth and delays the triggering of irrigation events in the early season. In contrast, the FAO-56 approach assumes a single soil layer that changes in thickness over the season to account for the progression of root growth to deeper depths. By relating the model's automatic irrigation management depth to simulated root growth, the model may be able to provide irrigation schedules that better mimic the timing of the FAO-56 schedule. Limitations in the automatic irrigation algorithm are also apparent in the specification of the irrigation volume to be applied. Currently, users have two choices: apply a single, user-specified volume on every irrigation date throughout the season, or fill the profile to the drained upper limit. Since irrigation volumes based on FAO-56 approaches during the field experiments refilled the profile to 110% of available storage capacity, it was not possible to specify this volume for automatic application without changing the model code. This resulted in more frequent and lower volume irrigations scheduled by the model from 90 to 130 DAP as compared to the FAO-56 schedule. The last recommendation for improvement of the automatic irrigation routine involves the simulation of late season irrigations. Realistically, a grower's last irrigation management decision will include an assessment of the crop's progression to harvest maturity and how much water is needed to "finish off" the crop. Currently, the automatic irrigation routine is based only on soil water contents, and the progression of crop development to maturity is not considered. This may result in the simulation of unrealistic and unneeded irrigations in the late season, as demonstrated by the simulated irrigation event 161 DAP in 2003-2004, which was 6 days before harvest. Until improvements are made in the automatic irrigation routine of the model, users should carefully examine how realistically the model is scheduling irrigations for their particular environment.

Although the effects of the model's automatic irrigation schedule on crop yield, ET, and deep seepage cannot be verified without further field investigation, a comparison of the simulated effects of the two irrigation schedules on these variables demonstrates that improvements in crop water management may be possible without substantial yield impacts (table 6). Use of model-based irrigation schedules reduced applied irrigation volumes from 12.3% to 46.1% as compared to the FAO-56 schedule. Greater reductions in irrigation volume were generally noted for the sparse population and low nitrogen treatments because the model accounts for the effects of these factors on water requirements whereas standard FAO-56 methods do not. According to the simulations, the reductions in irrigation volume were not accompanied by substantial changes in wheat yield. The greatest yield reduction was 5.1% for the FSH treatment in 2003-2004, but other treatments demonstrated a yield increase in response to the model-based irrigation schedule. Reductions in applied irrigation volume also led to reduced ET, with the exception of the FDH treatment in the 2003-2004 season. Lower soil water contents due to reduced irrigations may have led to

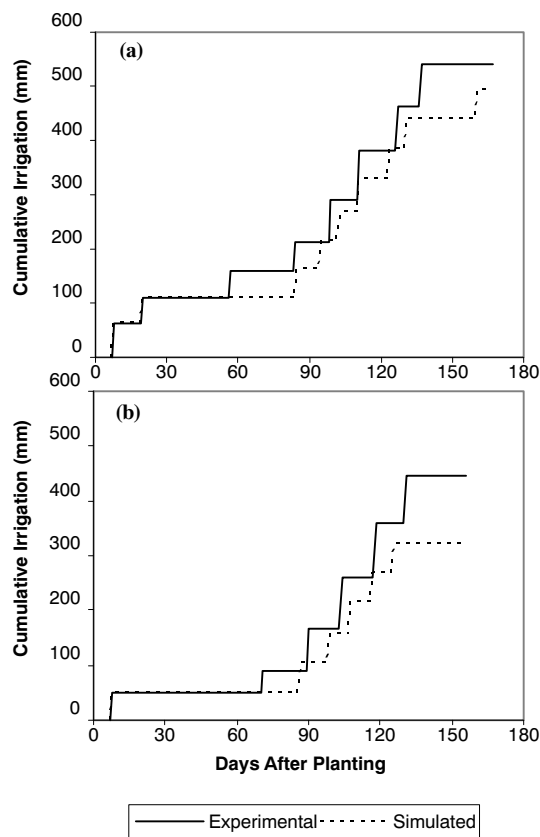


Figure 9. Irrigation requirements as computed using FAO-56 methods during field experimentation and simulated irrigation requirements using the model's automatic irrigation algorithm for the FAO-56, typical population, high nitrogen rate (FTH) treatment in the (a) 2003-2004 and (b) 2004-2005 FISE wheat experiments.

Table 6. Percent difference between simulation results when using the model's automatic irrigation schedule instead of the schedule devised using FAO-56 methods during the field experiments. Irrigation volumes, evapotranspiration, and deep seepage for these calculations were computed from emergence to physiological maturity.^[a]

	2003-2004 Experiment				2004-2005 Experiment			
	I	Y	ET	SP	I	Y	ET	SP
FSH	-37.6	-5.1	-9.2	0.0	-32.3	-0.1	-0.6	-71.4
FSL	-37.6	-0.6	-6.3	0.0	-46.1	1.1	-10.0	-72.4
FTH	-23.0	2.4	-4.8	0.0	-31.3	-0.1	-3.4	-58.3
FTL	-24.4	-0.2	-1.7	0.0	-31.6	0.6	-0.8	-68.1
FDH	-12.3	9.0	3.1	0.0	-31.6	-0.1	-4.9	-51.9
FDL	-25.8	2.1	-0.3	0.0	-30.0	0.6	-2.1	-66.7

[a] All values in %: I = irrigation volume, Y = wheat yield, ET = evapotranspiration, and SP = deep seepage

deeper root growth and uptake of nitrogen from deeper soil layers, which increased biomass growth, yield, and ET for this treatment. Substantial reductions in deep seepage were noted in the 2004-2005 season, but the model continued to simulate no deep seepage in 2003-2004 under the model-based irrigation schedule. These results encourage further investigation into the use of systems approaches to understand the effects of water management on crop production, such that appropriate decision tools can be developed to address water management objectives at field-level and regional scales.

CONCLUSIONS

- After a thorough evaluation of CSM-CROPSIM-CERES-Wheat, the model was able to reasonably quantify wheat development, growth, and yield responses to within-season variability in plant population and nitrogen application rate and to seasonal variation in weather and management practices.
- The CSM soil water component was able to reasonably quantify changes in soil water contents in eight soil layers in response to variation in irrigation and precipitation over two growing seasons.
- Incorporation and calibration of the EORATIO parameter, for adjusting potential ET simulations based on simulated LAI, was necessary for CSM-CROPSIM-CERES-Wheat to reasonably simulate actual ET for the arid conditions of this central Arizona study. Further model development, such as incorporation of more physically based energy balance algorithms, is warranted to improve the model's ability to simulate ET without empirical adjustments such as the EORATIO.
- Given that deep seepage for agricultural systems in arid environments may be within the expected range of error for simulations of ET and soil water storage, the reliability of the deep seepage simulation may be questionable until better simulation techniques are available for simulating these other aspects of the water balance.
- Until the CSM automatic irrigation algorithms are improved further, users should scrutinize how realistically the model can produce irrigation schedules for their particular environment.
- Further investigation is warranted into the use of crop systems models to evaluate water management alternatives for irrigated agricultural systems.

ACKNOWLEDGEMENTS

The authors express great appreciation to the people who supported the collection of a magnificent dataset for model testing during the intensive FISE wheat field campaigns, including C. Arterberry, A. Ashley, M. Conley, R. Jackson, S. Johnson, W. Luckett, S. Maneely, D. Powers, S. Richards, and R. Rokey of the USDA-ARS U.S. Arid-Land Agricultural Research Center, and M. Hartman, D. Langston, C. Jones, G. Main, C. O'Brien, and S. Hahnke of the University of Arizona Maricopa Agricultural Center.

REFERENCES

- Allen, R. G., L. S. Pereira, D. Raes, and M. Smith. 1998. Crop evapotranspiration: Guidelines for computing crop water requirements. FAO Irrigation and Drainage Paper 56. Rome, Italy: Food and Agriculture Organization of the United Nations.
- Arora, V. K., H. Singh, and B. Singh. 2007. Analyzing wheat productivity responses to climatic, irrigation, and fertilizer-nitrogen regimes in semi-arid sub-tropical environment using the CERES-Wheat model. *Agric. Water Mgmt.* 94(1-3): 22-30.
- Bannayan, M., N. M. J. Crout, and G. Hoogenboom. 2003. Application of the CERES-Wheat model for within-season prediction of winter wheat yield in the United Kingdom. *Agron. J.* 95(1): 114-125.
- Cai, J. B., Y. Liu, D. Xu, P. Paredes, and L. S. Pereira. 2009. Simulation of the soil water balance of wheat using daily weather forecast messages to estimate the reference evapotranspiration. *Hydrol. and Earth System Sci.* 13(7): 1045-1059.
- Chipanshi, A. C., E. A. Ripley, and R. G. Lawford. 1999. Large-scale simulation of wheat yields in a semi-arid environment using a crop-growth model. *Agric. Systems* 59(1): 57-66.
- Chow, V. T., D. R. Maidment, and L. W. Mays. 1988. *Applied Hydrology*. New York, N.Y.: McGraw-Hill.
- Eitzinger, J., M. Trnka, J. Hösch, Z. Žalud, and M. Dubroský. 2004. Comparison of CERES, WOFOST, and SWAP models in simulating soil water content during growing season under different soil conditions. *Ecol. Modelling* 171(3): 223-246.
- George, B. A., N. S. Raghuwanshi, and R. Singh. 2004. Development and testing of a GIS integrated irrigation scheduling model. *Agric. Water Mgmt.* 66(3): 221-237.
- Guerra, L. C., G. Hoogenboom, V. K. Boken, J. E. Hook, D. L. Thomas, and K. A. Harrison. 2004. Evaluation of the EPIC model for simulating crop yield and irrigation demand. *Trans. ASAE* 47(6): 2091-2100.
- Hunsaker, D. J., E. M. Barnes, T. R. Clarke, G. J. Fitzgerald, and P. J. Pinter Jr. 2005. Cotton irrigation scheduling using remotely sensed and FAO-56 basal crop coefficients. *Trans. ASAE* 48(4): 1395-1407.
- Hunsaker, D. J., G. J. Fitzgerald, A. N. French, T. R. Clarke, M. J. Ottman, and P. J. Pinter Jr. 2007a. Wheat irrigation management using multispectral crop coefficients: I. Crop evapotranspiration prediction. *Trans. ASABE* 50(6): 2017-2033.
- Hunsaker, D. J., G. J. Fitzgerald, A. N. French, T. R. Clarke, M. J. Ottman, and P. J. Pinter Jr. 2007b. Wheat irrigation management using multispectral crop coefficients: II. Irrigation scheduling performance, grain yield, and water use efficiency. *Trans. ASABE* 50(6): 2035-2050.
- Itier, B., F. Maraux, P. Ruelle, and J. M. Deumier. 1996. Applicability and limitations of irrigation scheduling methods and techniques. In *Irrigation Scheduling: From Theory to Practice, Proc. ICID/FAO Workshop on Irrigation Scheduling*. Rome, Italy: Food and Agriculture Organization of the United Nations. Available at: www.fao.org/docrep/w4367e/w4367e04.htm. Accessed 10 June 2008.
- Jones, J. W., G. Hoogenboom, C. H. Porter, K. J. Boote, W. D. Batchelor, L. A. Hunt, P. W. Wilkens, U. Singh, A. J. Gijssman, and J. T. Ritchie. 2003. The DSSAT cropping systems model. *European J. Agron.* 18(3-4): 235-265.
- Loague, K., and R. E. Green. 1991. Statistical and graphical methods for evaluating solute transport models: Overview and application. *J. Contaminant Hydrol.* 7(1-2): 51-73.
- Lobell, D. B., and J. I. Ortiz-Monasterio. 2006. Evaluating strategies for improved water use in spring wheat with CERES. *Agric. Water Mgmt.* 84(3): 249-258.
- Nain, A. S., V. K. Dadwal, and T. P. Singh. 2004. Use of CERES-Wheat model for wheat yield forecast in central Indo-Gangetic Plains of India. *J. Agric. Sci.* 142(1): 59-70.
- Nash, J. E., and J. V. Sutcliffe. 1970. River flow forecasting through conceptual models: I. A discussion of principles. *J. Hydrol.* 10(3): 282-290.
- Pereira, L. S., T. Oweis, and A. Zairi. 2002. Irrigation management under water scarcity. *Agric. Water Mgmt.* 57(3): 175-206.
- Pinter, Jr., P. J., B. A. Kimball, G. W. Wall, R. L. LaMorte, D. J. Hunsaker, F. J. Adamsen, K. F. A. Frumau, H. F. Vugts, G. R. Hendrey, K. F. Lewin, J. Nagy, H. B. Johnson, F. Wechsung, S. W. Leavitt, T. L. Thompson, A. D. Matthias, and T. J. Brooks. 2000. Free-air CO₂ enrichment (FACE): Blower effects on wheat canopy microclimate and plant development. *Agric. and Forest Meteorology* 103(4): 319-333.
- Post, D. F., C. Mack, P. D. Camp, and A. S. Suliman. 1988. Mapping and characterization of the soils on the University of Arizona Maricopa Agricultural Center. In *Proc. Hydrology and Water Resources in Arizona and the Southwest*, 49-60. Tucson, Ariz.: University of Arizona.

- Rinaldi, M. 2004. Water availability at sowing and nitrogen management of durum wheat: A seasonal analysis with the CERES-Wheat model. *Field Crops Res.* 89(1): 27-37.
- Santhi, C., R. S. Muttiah, J. G. Arnold, and R. Srinivasan. 2005. A GIS-based regional planning tool for irrigation demand assessment and saving using SWAT. *Trans. ASAE* 48(1): 137-147.
- Sau, F., K. J. Boote, W. M. Bostick, J. W. Jones, and M. I. Mínguez. 2004. Testing and improving evapotranspiration and soil water balance of the DSSAT crop models. *Agron. J.* 96(5): 1243-1257.
- Schaap, M. G., F. J. Leij, and M. T. Van Genuchten. 2001. ROSETTA: A computer program for estimating soil hydraulic parameters with hierarchical pedotransfer functions. *J. Hydrol.* 251(3-4): 163-176.
- Stockle, C. O., and L. G. James. 1989. Analysis of deficit irrigation strategies for corn using crop growth simulation. *Irrig. Sci.* 10(2): 85-98.
- Tubiello, F. N., C. Rosenzweig, B. A. Kimball, P. J. Pinter, Jr., G. W. Wall, D. J. Hunsaker, R. L. LaMorte, and R. L. Garcia. 1999. Testing CERES-Wheat with free-air carbon dioxide enrichment (FACE) experiment data: CO₂ and water interactions. *Agron. J.* 91(2): 247-255.
- Zadoks, J. C., T. T. Chang, and C. F. Konzak. 1974. A decimal code for the growth stages of cereals. *Weed Res.* 14(6): 415-421.